Poster 27

Virtual screening and biophysical studies lead to HSP90 inhibitors

Daniel Moscoh Ayine-Tora
Jóhannes Reynisson, Ivanhoe K.H. Leung, Renjie Huang, Nasri Muhammad Rosdi, Yu Li

Heat shock protein 90 (HSP90) is a molecular chaperone that plays important functional roles in cells.[1] The chaperone activity of HSP90 is regulated by the hydrolysis of ATP at the protein's N-terminal domain. HSP90, in particular, the N-terminal domain, is a current inhibition target for therapeutic treatments of cancers.[2, 3] Virtual screening, thermal shift assaying and protein NMR spectroscopy have been used to identify HSP90 inhibitors that contain the resorcinol structure. The resorcinol scaffold can be found in a class of HSP90 inhibitors that are currently undergoing clinical trials. Molecular modelling shows the active ligands form hydrogen bonds with Asn37, Lys44, Asp79, Glu88 and Thr171. The proved success of the resorcinol moiety in HSP90 inhibitors validates this combined virtual screen and biophysical technique approach, which can be applied for future inhibitor discovery work for HSP90 as well as other targets.

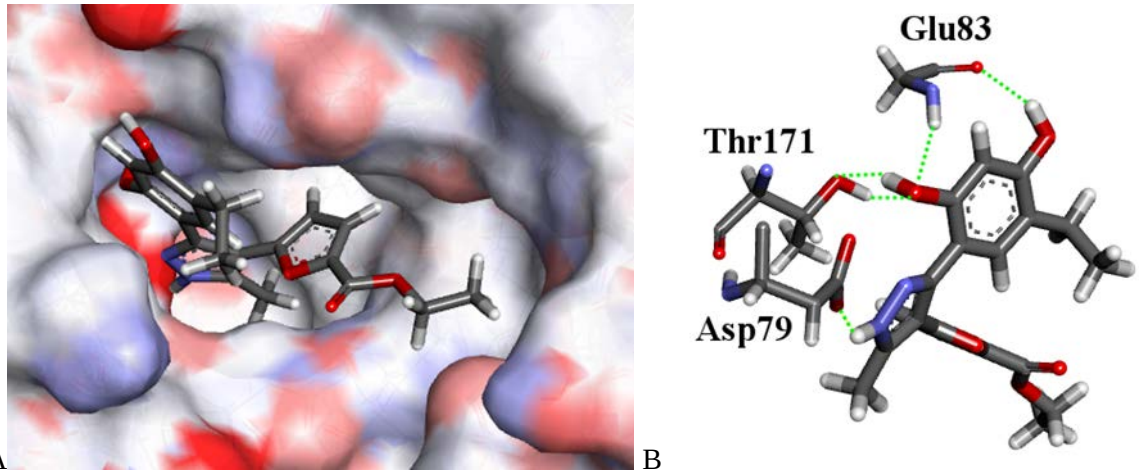

Figure 1. The docked configuration of **1** in the binding site of HSP90 (**A**) The protein surface is rendered. Red depicts a negative partial charge on the surface, blue depicts positive partial charge and grey shows neutral/lipophilic areas. The ligand occupies the binding pocket. (**B**) Hydrogen bonds are shown as green lines between ligand **1** and the amino acids Asp79,Glu83 and Thr171 for ChemScore configuration.

1 Wiech, H.; Buchnerij, J. *Nature* **1992**, *358*, 9.
2 Trepel, J.; Mollapour, M.; Giaccone, G.; Neckers, L. *Nature reviews cancer* **2010**, *10*, 537.
3 Isaacs, J. S.; Xu, W.; Neckers, L. *Cancer cell* **2003**, *3*, 213.

Poster 28

Synthesis of Biodegradable Antimicrobial Polymers with High Selectivity

Chloe Cho[1], Chao Liang[1], Janesha Perera[2], Viji Sarojini[1], Ralph Cooney[1], Margaret Brimble[1], Simon Swift[2] and Jianyong Jin[1*]

[1]School of Chemical Sciences, The University of Auckland
[2]Department of Molecular Medicine and Pathology, The University of Auckland

A biodegradable aliphatic polycarbonate was synthesised via ring-opening polymerisation of six-membered cyclic carbonate monomer with terminal alkyne side chain.[1] The positively charged guanidine group was attached to the polymer backbone via the Cu(I)-catalysed alkyne-azide cycloaddition click reaction. Guanidine polycarbonates with three different molecular weights were synthesised to investigate the molecular weight effect of these polymers on antimicrobial activity and cytotoxicity.

As a result, antimicrobial inhibition assays of different molecular weight guanidine polycarbonates killed a broad spectrum of microbes with low toxicity (Table 1). The lowest molecular weight polymer showed stronger activity against *E.coli* with the minimum inhibitory concentration (MIC) of 40 μg/mL than previously reported guanidine functionalised polymethacrylates[2] (MIC > 1500 μg/mL). This was an interesting finding because traditionally, inhibition of Gram-negative bacteria is more difficult than that of Gram-positive bacteria due to the more complex cell wall membrane structure.[3]
The lytic activity of the polymers was examined against mammalian red blood cells and all polymers showed low toxicity (hemolysis % < 20%) at high concentration.

Membrane disruption of bacterial cell membranes was identified through field emission scanning electron microscopy (FE-SEM) and further study on the antimicrobial action of these cationic polymers will be reported in due time.

		MIC (μg/mL)				
Polymer	DP	*E.coli* (Gram –ve)	*P.aeruginosa* (Gram –ve)	*S.aureus* (Gram +ve)	*C.albicans* (Fungus)	HC_{50} (μg/mL)
PG-1	20	40	40	80	80	>1280
PG-2	40	40	40	160	160	>1280
PG-3	80	40	80	160	320	>1280

Table 1. Antimicrobial (MIC) and hemolytic (HC_{50}) activities of guanidine polycarbonate series of polymers.

1. Pratt, R. C.; Nederberg, F.; Waymouth, R. M.; Hedrick, J. L. *Chem. Commun.* **2008**, 114-116.
2. Locock, K. E.; Michl, T. D.; Valentin, J. D.; Vasilev, K.; Hayball, J. D.; Qu, Y.; Traven, A.; Griesser, H. J.; Meagher, L.; Haeussler, M. *Biomacromolecules* **2013,** *14*, 4021-31.
3. Beveridge, T. J. *Journal of bacteriology* **1999,** *181*, 4725-4733.

Poster 29

Chemistry of sulfur-functionalized osmabenzenes

Terence M. Christy*
L. James Wright
University of Auckland, Private Bag 32019, Auckland, New Zealand
*tchr010@aucklanduni.ac.nz

Metallabenzenes are a relatively new class of compounds, first being hypothesized in 1979 by Thorn and Hoffman[1]. The first metallabenzene, an osmabenzene (**1**) was synthesized in 1982. These compounds have attracted significant attention and show both similarities and differences in reactivity, when compared to that of traditional aromatic compounds.[2, 3]

While research into the reactivity of these compounds is still in its infancy, some definite parallels with their organic counterparts have emerged. Protonation of the S atom in **1** gives the osmathiol product without disruption of the aromaticity of the metallabenzene ring. When an isothiocyanate ligand is present at the metal centre, the thiol substituted osmabenzene **2** can be oxidized by thiocyanogen to the corresponding disulfide, **3**. An analogous reaction is observed for many organic aromatic thiols. The osmabenzene dimer **3** has been found to undergo electrophilic aromatic substitution reactions without cleavage of the S-S bond. Nitration under Menke conditions and bromination with pyridinium tribromide both resulted in substitution at the position para to the disulfide linkage, on both metallabenzene rings. The analogous iridabenzene dimer $[Ir(C_5H_4\{S\}\text{-}1)Cl_2(PPh_3)_2]_2$ can be prepared by treatment of the iridathiol $Ir(C_5H_4\{SH\}\text{-}1)Cl_2(PPh_3)_2$ with the oxidant I_2.

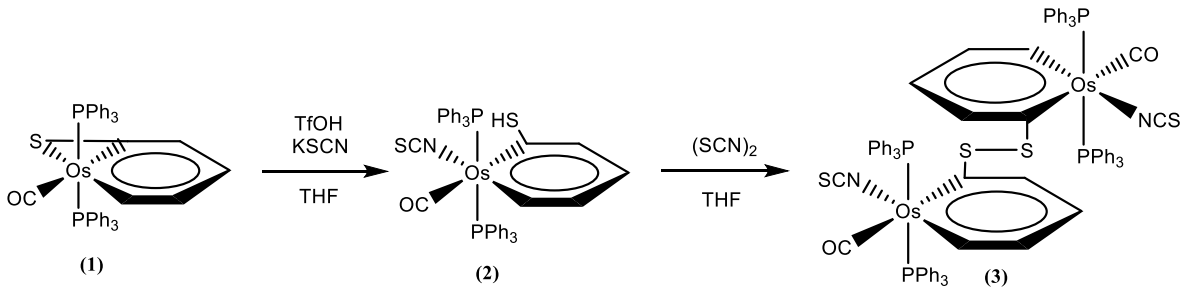

Figure 1. Synthetic scheme showing the oxidation of **2** to the corresponding disulfide **3**.

1. Thorn, D. L.; Hoffmann, R. *Nouv J Chim.* **1979**, 3, 39.
2. Chen, Jiangxi; Jia, Guochen Coord. Chem. Rev. **2013**, 257(17-18), 2491-2521.
3. Dalebrook, Andrew F.; Wright, L. James Adv. Organomet. Chem. **2012**, 60, 93-177.

Poster 30

Synthetic studies towards an enantiomeric pair of indole alkaloids isolated from the roots of *Isatis indigotica*

Emma K. Davison and Jonathan Sperry

The unnamed enantiomeric pair of indole alkaloids **1a** and **1b** were isolated from the roots of the herbaceous plant *Isatis indigotica* which is commonly used in Chinese traditional medicine.[1] These natural products contain a dihydrothiopyran and a 1,2,4-thiadiazole heterocycle, the latter being an exceptionally rare motif in Nature. Synthetic studies towards **1a** and **1b** will be discussed, whereby a late-stage intermolecular Heck reaction between **2** and **3** is proposed to construct the complete heteroaromatic framework of the natural products.

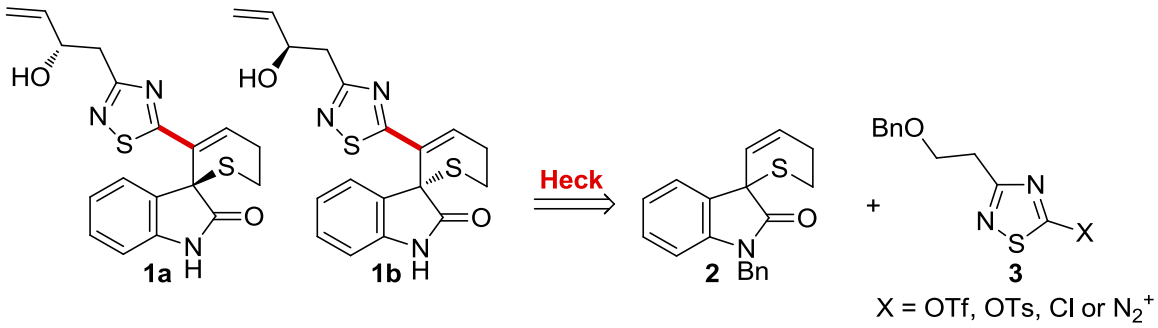

1. Chen, M.; Lin, S.; Li, L.; Zhu, C.; Wang, X.; Wang, Y.; Jiang, B.; Wang, S.; Li, Y.; Jiang, J.; Shi, J. *Org. Lett.* **2012**, *14*, 5668-5671

Poster 31

Development of Efficient Phosphors for NIR Upconversion

Aubrey Dosado
Geoffrey I.N. Waterhouse, Dongxiao Sun-Waterhouse

Crystal matrices doped with rare earth ions such as Yb^{3+}, Tm^{3+}, Er^{3+}, are capable of upconverting multiple low energy near-infrared (NIR) photons into visible and UV photons. NIR absorption (980 nm) by Yb^{3+} in $NaYF_4$:Yb,Tm leads to multiple UV-Vis emissions (Figure 1) due to coincidence of the ladder-like energy levels and f-f transitions of Yb^{3+} and Tm^{3+}.[1] This study systematically explored the effect of synthesis conditions and crystal morphology on the NIR upconversion performance of $NaYF_4$:Yb,Tm. These upconverters were prepared via hydrothermal treatment at 180 °C from metal nitrates (molar ratio Y:Yb:Tm = 80:20:0.5) and NaF, whilst varying pH and the structure regulating agents (citric acid and trisodium citrate).[2] Products were characterised by XRD, TEM, SEM, XPS and UV-Vis absorbance and luminescence measurements. NIR upconversion performance was observed to be highly dependent to crystal size and shape, with $NaYF_4$:$Yb_{0.20}$,$Tm_{0.05}$ prepared with citric acid showing the most intense emissions overall. Tethering these crystals to gold nanorods with a longitudinal surface plasmon resonance (LSPR) at ~980 nm is being attempted, to identify how plasmonic effects can influence upconversion.[1,3] Other upconverters such as rare earth doped $NaBiF_4$ analogues and metal organic frameworks (MOFs) are also being developed.[4,5]

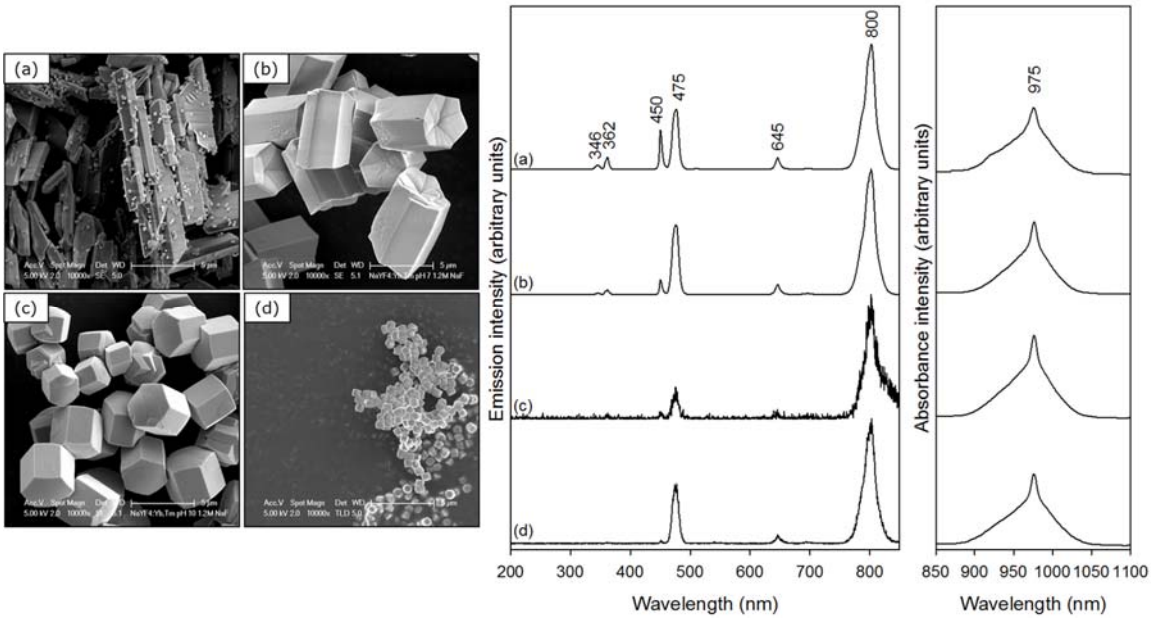

Figure 1. (left) SEM images of hexagonal phase $NaY_{0.80}F_4$:$Yb_{0.20}$, $Tm_{0.05}$ prepared with (a) citric acid (b) citric acid adjusted to pH 7, (c) citric acid adjusted to pH 10 and (d) trisodium citrate. (right) Corresponding emission and absorption spectra.

1. Wu, D. M.; García-Etxarri, A.; Salleo, A.; Dionne, J. A. *The Journal of Physical Chemistry Letters* **2014,** *5*, 4020-4031.
2. Jiang, T.; Qin, W.; Zhou, J. *Journal of Fluorine Chemistry* **2013,** *156*, 177-182.
3. Xu, Z.; Quintanilla, M.; Vetrone, F.; Govorov, A. O.; Chaker, M.; Ma, D. *Advanced Functional Materials* **2015,** *25*, 2950-2960.
4. Lei, P.; An, R.; Yao, S.; Wang, Q.; Dong, L.; Xu, X.; Du, K.; Feng, J.; Zhang, H. *Advanced Materials* **2017,** *29*.
5. Zhang, X.; Li, B.; Ma, H.; Zhang, L.; Zhao, H. *ACS Applied Materials & Interfaces* **2016,** *8*, 17389-17394.

Poster 32

Synthetic Studies Towards the Gombaspiroketals

Megan Jamieson
Daniel P. Furkert, Margaret A. Brimble

The gombaspiroketals were isolated from the marine sponge *Clathria gombawuiensis* off the coast of South Korea.[1] They are members of a diverse group of 6,6-spirocyclic sesterpenoid natural products biogenetically derived from the alotane skeleton, which includes the notably bioactive natural products of the alotaketal and phorbaketal families.[1-4] The gombaspiroketals exhibit a range of bioactivities including cytotoxicity and antibacterial activity.[1] As a part of ongoing interest within our group on synthetic approaches to spiroketal natural products, a total synthesis of the gombaspiroketals is envisioned which will allow full biological testing of these natural products.

Previous work in our group has established syntheses of γ-hydroxy carvone derivatives such as the allylsilane shown in blue. The current research towards the gombaspiroketals involves synthesis of an appropriate acetal fragment (black) to be coupled to the allylsilane (blue) *via* a Hosomi Sakurai reaction. Future work will investigate the oxidative radical spirocyclisation and further oxidative modifications to furnish the completed natural products.

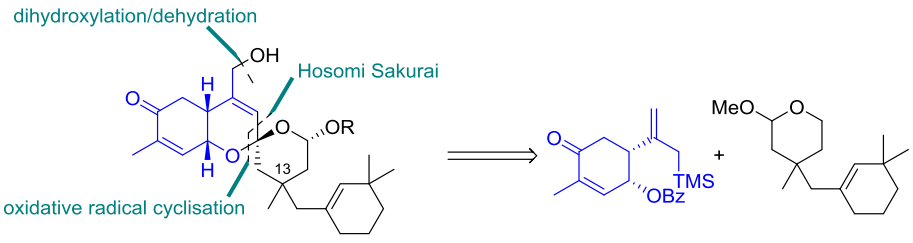

Gombaspiroketal A: R = Me C13 *R*
Gombaspiroketal B: R = Me C13 *S*
Gombaspiroketal C: R = H C13 *R*

1. Woo, J.; Kim, C.; Kim, S.; Kim, H.; Oh, D.; Oh, K.; Shin, J. *Org. Lett.* **2014**, *16*, 2826-2829.
2. Rho, J.; Hwang, B. S.; Sim, C. J.; Joung, S.; Lee, H.; Kim, H. *Org. Lett.* **2009**, *11*, 5590-5593.
3. Forestieri, R.; Merchant, C. E.; de Voogd, N. J.; Matainaho, T.; Kieffer, T. J.; Andersen, R. J. *Org. Lett.* **2009**, *11*, 5166-5169.
4. Byun, M. R.; Lee, C. H.; Hwang, J.; Kim, A. R.; Moon, S. A.; Sung, M. K.; Roh, J.; Hwang, E. S.; Hong, J. *Eur. J. Pharmacol.* **2013**, *718*, 181-187.

Poster 33

Subcritical water extraction of phenolic compounds from kiwifruit processing by-product

Hamid kheirkhah[1], Saeid Baroutian[2], Brent R. Young[2], Siew-Young Quek[1]

[1]Department of Chemical Sciences, Faculty of Science, The University of Auckland 1010, Auckland, New Zealand

[2]Department of Chemical & Materials Engineering, Faculty of Engineering, The University of Auckland, Auckland 1023, New Zealand

Abstract:

This study was designed to investigate the recovery of phenolic compounds from kiwifruit pomace using subcritical water extraction (SWE). The effect of key operating conditions was determined by altering the extraction temperature (170–225 ºC) and time (10–180 min) under a constant high pressure (50 bar). The total phenolic and flavonoid content, as well as the antioxidant capacity of extracts, were assessed. To evaluate the feasibility of SWE technique the results were compared with those obtained using conventional solvent extractions. High recovery of phenolic compounds (60.53 mg CaE/ g DW) was gained at 200 °C and extraction time of 90 min presented 20-, 15-,7.5-fold higher value than ethanol, methanol and acetone extraction respectively. HPLC-DAD analyses were performed to identify individual phenolic compounds which protocatechuic acid, (+)-catechin, chlorogenic acid, *p*-coumaric acid and caffeic acid were found to be the most abundant phenolic compounds. Furthermore, the formation of Maillard reaction products during SWE was investigated, and the level of 5-hydroxymethylfurfural (5-HMF) was determined using HPLC. The outcomes of this study indicated a potential formation of antioxidants from natural phenolic compounds and subcritical water is an effective solvent to extract certain phenolic compounds, in many cases more advantageous than conventional techniques.

Keywords: Kiwifruit pomace; subcritical water extraction; phenolic compounds; 5-HMF; solvent extraction.

Poster 34

Total synthesis of callyspongiolide

Kwangyoon (Jason) Ko
Daniel P. Furkert and Margaret A. Brimble

Callyspongiolide (**1**) is a novel 14-membered macrolide isolated from the Indonesian marine sponge *Callyspongia sp.* Callyspongiolide possesses a unique conjugated ynediene moiety (C14-C19) that is unprecedented among the natural products reported to date. Preliminary *in vitro* studies of callyspongiolide showed antiproliferative activities against human Jurkat J16 T and Ramos B lymphocytes with IC_{50} values of 70 nM and 60 nM respectively. Interestingly, the activity of callyspongiolide did not diminish on parallel treatment with a caspase inhibitor, QVD-OPh, suggesting a caspase-independent mode of induction of cell death.[1]

Recently, studies by Zhou *et al.*[2] have shown that the previously undefined stereochemistry at C21 position of callyspongiolide is *R*. Further, the absolute stereochemistry of the macrolide region was in fact the antipode of the initially assigned structure (shown in figure 1) at the time of isolation.

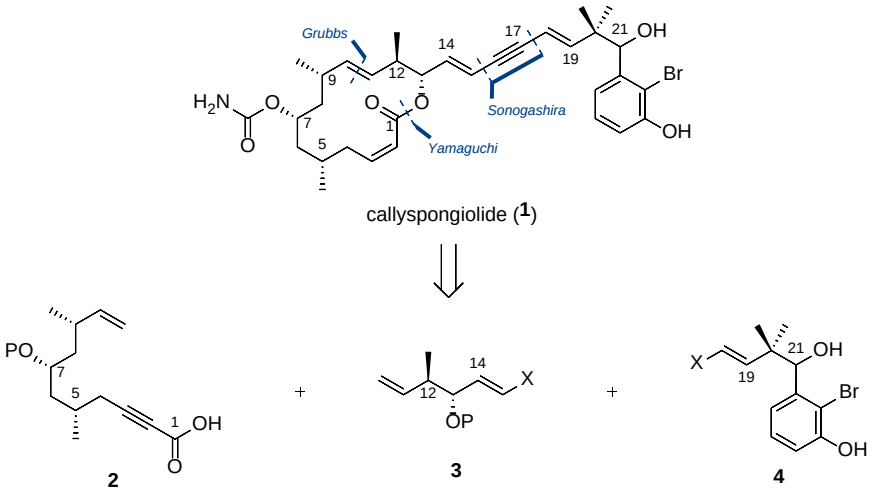

Figure 1. Retrosynthetic analysis of callyspongiolide (**1**).

Our synthetic approach toward callyspongiolide involves a convergent synthesis strategy, generating the key fragments from readily available starting materials that are coupled together in later stages via ring closing metathesis to furnish the macrolide, followed by a Sonogashira coupling to append the aromatic side chain.

1. Pham, C.-D.; Hartmann, R.; Böhler, P.; Stork, B.; Wesselborg, S.; Lin, W.; Lai, D.; Proksch, P. *Org. Lett.* **2014**, *16* (1), 266–269.
2 Zhou, J.; Gao, B.; Xu, Z.; Ye, T. *J. Am. Chem. Soc.* **2016**, *138*, 6948-6951.

Poster 35

Physicochemical properties and molecular structures of kiwifruit starches

Dongxing Li
Supervisor: Dr Fan Zhu

Three varieties of golden kiwifruit (Actinidia chinensis) (Gold3, Gold9 and Hort16A) were collected at the commercial harvesting time, and physicochemical properties and molecular structures of starches from core and outer pericarp were studied. Starch contents (dry weight basis) in outer pericarp and core tissues ranged from 38.6 to 51.8% and 34.6 to 40.7%, respectively. All the kiwifruit starches showed B-type polymorph. Compared to the outer pericarp starches, amylose content and enzyme susceptibility of core starches were higher, and the degree of crystallinity, granule size and gelatinization parameters of core starches were somewhat lower. The core starches have more long unit chains of both amylopectins and their φ, β-limit dextrins than their outer pericarp starches. Short B-chain of the amylopectin from outer pericarp is ~ 3% higher that of the core. Overall, the physicochemical properties and structure of starches from outer pericarp and core are different in a golden kiwifruit. This study revealed the unique properties of kiwifruit starch among various types of starches and may provide a structural basis to investigate the starch degradation in kiwifruit, which is curial for prolonging the shelf life and final taste of the fruit.

Poster 36

Surface Presented Biocides- Anchored Quaternary Ammonium Salts on Quartz

Rachel Tessy Mathew
Ralph Cooney, Jenny Malmstrom

A commercially established EPA and FDA approved siloxane surface-anchored quaternary ammonium salt with known anti-bacterial potencies and properties, has been chemisorbed onto a quartz substrate. The AQAS biocide adsorbate consists of a quaternary nitrogen centre and a C_{18} alkyl chain both of which is involved in the proposed lysis potency mechanism. The surface coverage of the resultant AQAS stable layer which includes a monolayer (2-3nm) and multi-layering was measured using Atomic Force Microscopy (AFM). The extent of multi-layering was found to be dependent on the AQAS solution concentration used in the preparation of the surface layers. An angular dependent X-ray Photoelectron Spectroscopy (XPS) study revealed the existence of two N (1s) signals at about 402 and 399eV, with only the former exhibiting angular dependence. This angular dependent XPS signal at 402eV was assigned to the first monomolecular layer with an assigned perpendicular orientation and height determined primarily by the AQAS siloxane covalent anchoring to the surface[1]. The non-angular dependant N (1s) signal is attributed to the disordered AQAS multi-layers. Preliminary studies of bacteria on these AQAS surfaces revealed perturbations[2] on the top surface of the cells, margins of Staphylococcus *aureus* cells and evident degradation of *Escherichia coli* of the peripheral cells, which are all consistent with lysis potency[3, 4].

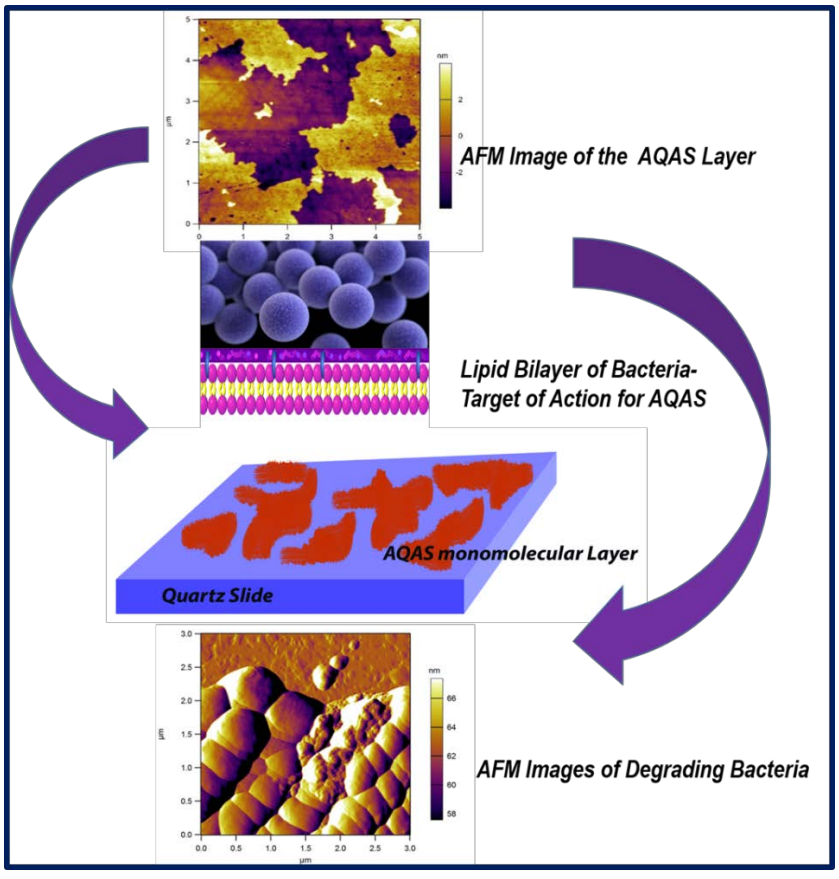

Figure 1. AQAS bonding onto quartz surfaces showing interpenetrating network forming a film structure as evident from the AFM image (below) and perturbations of S.aureus cells on the AQAS surface (AFM amplitude image above)

References

(1) Yarovsky, I.; Aguilar, M.; Hearn, M. T. Influence of the Chain Length and Surface Density on the Conformation and Mobility of N-Alkyl Ligands Chemically Immobilized Onto a Silica Surface. *Anal. Chem.* **1995**, *67*, 2145-2153.

(2) Yang, X.; Yang, W.; Wang, Q.; Li, H.; Wang, K.; Yang, L.; Liu, W. Atomic Force Microscopy Investigation of the Characteristic Effects of Silver Ions on Escherichia Coli and Staphylococcus Epidermidis. *Talanta* **2010**, *81*, 1508-1512.

(3) Stephenson, R. E.; Gutierrez, D.; Peters, C.; Nichols, M.; Boles, B. R. Elucidation of Bacteria found in Car Interiors and Strategies to Reduce the Presence of Potential Pathogens. *Biofouling* **2014**, *30*, 337-346.

(4) D'Antonio, N. N.; Rihs, J. D.; Stout, J. E.; Victor, L. Y. Computer Keyboard Covers Impregnated with a Novel Antimicrobial Polymer significantly Reduce Microbial Contamination. *Am. J. Infect. Control* **2013**, *41*, 337-339.

Poster 37

Low-Frequency Ultrasound Homogenization of Cream

Fithri Choirun Nisa
Yacine Hemar, Conrad Perera

Homogenization of cream, by reducing fat globule size, can be utilized to inhibit creaming. For cream with fat contents higher than 17% (volume) cannot be homogenized with satisfactory results when conventional methods are used.[1] Ultrasonication has been identified as a particularly promising technology for homogenization of dairy products.[2] Previous study on ultrasonication of cream under cold condition (<10°C) showed that it can reduce the fat globule. However, ultrasonication for 30s resulted in the formation of coalesced fat globules forming large fat clusters.[3] Results on the ultrasound homogenization of cream at 20kHz with various fat content (5-30%) and temperatures (2-60°C) are reported. The results show that ultrasonication can reduce the fat globule size, although it results in the formation of fat clusters at low temperature (<20°C) and short time (<1min), but at longer time, fat clusters can be broken. Microstructure of solid fraction showed that there was partial fat coalescence and formation of double emulsions. Fatty acid composition revealed that long-chain and medium-chain fatty in solid fraction was higher compared to those present in the liquid fraction. Ultrasound homogenization at temperature ≥20°C and the addition of SDS can prevent the formation of fat clusters even at low temperature.

1. Köhler, K., Aguilar, F. A., Schubert, H., Hensel, A., Schubert, K., & Schuchmann, H. P. *Chemical Engineering & Technology* **2008***, 31*(12), 1863-1868.
2. Ashokkumar, M., Bhaskaracharya, R., Kentish, S., Lee, J., Palmer, M., & Zisu, B. *Dairy Science & Technology* **2010***, 90*(2-3), 147-168.
3. Chandrapala, J., Ong, L., Zisu, B., Gras, S. L., Ashokkumar, M., & Kentish, S. E. *Innovative Food Science & Emerging Technologies* **2016***, 33*, 298-307.

Poster 38

Synthetic Studies Towards The Total Synthesis of Opaliferin

Opiyo O. George
Dist. Prof. Margaret A. Brimble, Dr. Daniel P. Furkert

Opaliferin (**1**), a bioactive polyketide metabolite with a novel C_{19} skeleton, was recently isolated from the insect pathogenic fungus of the genus *Cordyceps* in Japan, and reported to exhibit moderate anti-cancer activity *in vitro* against three tumour cell lines.[1] The structurally related natural product, oudenone, exhibits inhibitory activity against tyrosine hydroxylase and a strong hypotensive effect,[2] an indication that (**1**) may exhibit other bioactive properties that are yet unknown. Synthesis will facilitate full biological screening and determination of potential structure-activity relationships.

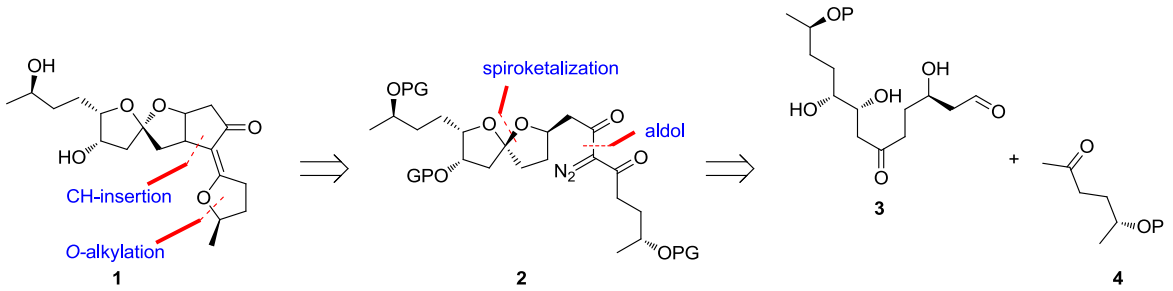

Figure 1. Retrosynthesis of opaliferin

Our initial strategy is focused on synthesis of the carbon framework (**2**) from chiral building blocks (**3** and **4**). The 5,5-spiroketal core is envisaged to be prepared from a dihydroxyketone precursor, while assembly of the fused cyclopentanone ring system by carbene C-H insertion will initially be investigated., *O*-alkylation will be used to provide the tetrahydrofuran ring fragment, [4] thus completing the total synthesis of **1**.

1. Grudniewska A.; Hayashi, S.; Shimizu, M.; Kato, M.; Suenaga, M.; Imagawa, H.; Ito, T.; Asakawa, Y.; Ban, S.; Kumada, T.; Hashimoto, T.; Umeyama, A. *Organic Lett.* **2014,** *16*, 4695-4697.
2. (a) Ohno, M.; Okamoto, M.; Kawabe, N. *J. Am. Chem. Soc.* **1971,** *93*, 1285-1286. (b) Umezawa, H.; Takeuchi, T.; Iinuma, H.; Suzuki, K.; Ito, M.; matsukazi, M. *J. Antibiot.* **1970,** *23*, 514-518.
3. Brimble, M. A.; Finch, O. C.; Heapy, A. M.; Fraser, J. D.; Furkert, D. P.; O'Conner, P. D. *Tetrahedron* **2011,** *67*, 995-1001.
4. Sakai, T.; Iwata, K.; Utaka, M.; takeda, A. *Bull. Chem. Soc. Jpn.* **1987,** *60*, 1161-1162.

Poster 39

Design, Synthesis and Biological Evaluation of Peptide based Inhibitors of Histone Deacetylases implicated in Cancer

Kamal Deepakbhai Patel
Viji Sarojini, Zimei Wu, Manju Kanamala

Cancer is considered to be the result of alterations in genetic and genomic modifications such as amplification, translocation, deletions and point mutations. However, apart from genetic modifications, epigenetic modifications also play important roles in cancer development.[1] Particularly implicated in epigenetic modifications resulting in malignancy are the enzymes histone deacetylases (HDACs) and Sirtuins. HDACs are upregulated in neuroblastoma and acute myeloid leukaemia (AMV). While inhibitors of these enzymes have been researched on, gaining selective inhibition of HDAC8 or SIR2 is important mainly because of their role in neuroblastoma development and only few selective inhibitors of HDAC8 and SIRT2 available till date. The development of selective inhibitors of these enzymes thus holds promise in cancer therapy. SIRT2 are ATP dependent enzymes, whereas HDAC8 enzymes are metallo-proteins and, in particular, require Zn ions for their activity (Figure 1). Taking into consideration the unique structural features of these enzymes, we have designed peptide derivatives as potential inhibitors of these enzymes.[2] Head-to tail cyclization and CPP conjugation of the linear peptides has been undertaken to minimise the inherent poor bio-availability issues of linear peptides. This study will present the syntheses and evaluation of anti-cancer properties of designed peptide based inhibitors targeting HDAC8 and SIRT2.

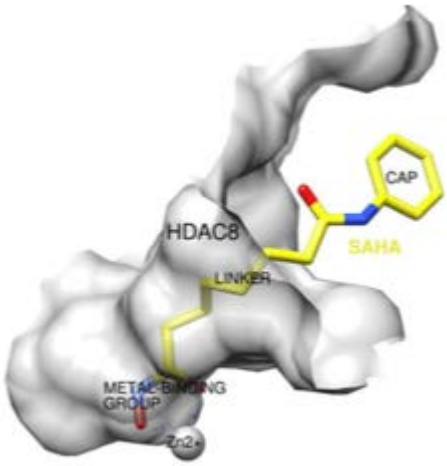

Figure 1: Crystal structure of Suberoylhydroxamic acid (SAHA), an HDAC inhibitor, bound to HDAC8 enzyme.

1. Johnstone, R. W. "Histone-deacetylase inhibitors: novel drugs for the treatment of cancer." Nat Rev Drug Discov, 2002.

2. Balasubramanian, S., J. Ramos, et al. A novel histone deacetylase 8 (HDAC8)-specific inhibitor PCI-34051 induces apoptosis in T-cell lymphomas. Leukemia., 2008.

Poster 40

Molecular Modelling and Virtual Screening for Isocitrate lyase I inhibitors

Krunal Patel
Ram Bhusal, Dr Ivanhoe Leung, Supervisor - Dr Jóhannes Reynisson

Mycobacterium tuberculosis can be latent in the human body, which can eventually be active tuberculosis. Isocitrate lyase (ICL) is the first enzyme of the glyoxylate cycle, which cleaves isocitrate to succinate and glyoxylate[1]. Oxaloacetate is biosynthesized in the process from both substrates. Oxaloacetate, which is a precursor of gluconeogenesis, it generates glucose molecules for the survival of Mycobacteria[2]. Till now, there are no inhibitors which can be used as drugs. Aim of the project to find potent inhibitors with high selectivity and less toxicity. Computation tools has been used to find the inhibitors, such as molecular modelling and virtual high throughput screening. Few promising compounds were identified through computation metrology. Biological studies has been done with few of them and still it is under process.

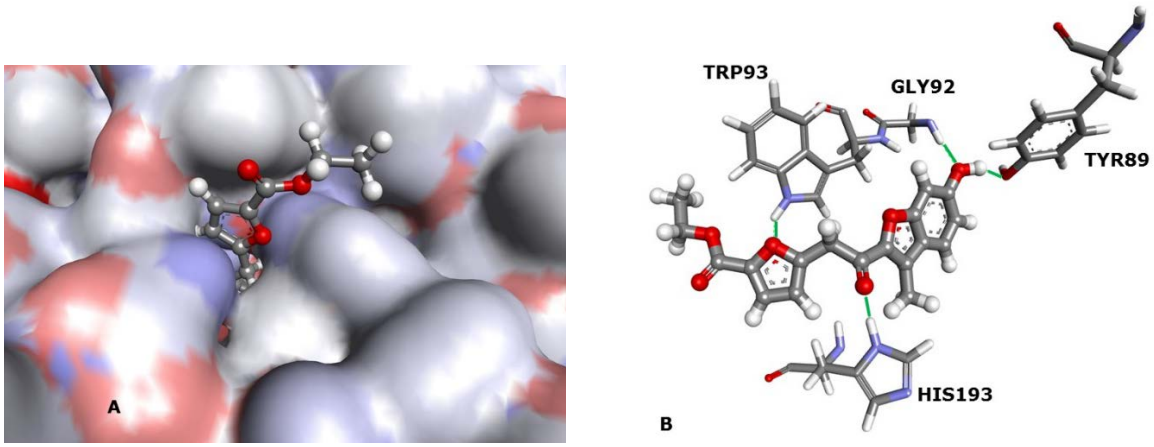

Figure 1. (A) The protein surface is rendered. The ligand occupies the binding pocket. (B) Hydrogen bonds are depicted as green lines between the ligand and the amino acids TRP93, HIS193, TYR89 and GLY92.

1. Wayne L. G.; Sohaskey C. D.; Nonreplicating persistence of Mycobacterium tuberculosis. Annu. Rev. Microbiol. 2001, 55, 139-63
2. Kratky M.; Vinsova J.; Advances in mycobacterial isocitrate lyase targeting and inhibitors. Current medicinal chemistry. 2012, 19, 6126-37.

Poster 41

Assessment of raw milk culture potential for the formation of flavour in cheese

Jessica Yoko Suda
Dr Bruno Fedrizzi[1], A/P Yacine Hemar[1], A/P Silas Villas-Boas[2], Dr Steffen Klaere[3]
[1] School of Chemical Sciences, [2] School of Biological Sciences, [3]Department of Statistics

The acceptability of dairy products by consumers rely mainly on their sensory attributes in which flavour plays a major role[1]. The typical aroma of cheese is the result of the combination and balance of a great number of volatile compounds present in specific ratio and concentration[2]. These compounds are originated by the action of microorganisms and their enzymes in milk giving rise to a complex range of volatile metabolites[3]. Thus, volatile organic compounds (VOC) can influence the relationship between production chain and consumer acceptability. In other words, the characteristics of the milk from different farms affect the sensory quality of matured cheese, the VOC profile in particular[1]. In this way, the aim was to study the potential aroma profile produced using raw cow's milk endogenous microflora as adjunct culture and to determine the resulting volatile signature. The study was conducted using a cheese-like model added with commercial starter culture and raw milk. The cheese-like model was aged for 4 weeks and analysed for volatile composition using HE-SPME and GCMS. The measured data were analysed using an untargeted approach.

1. Bergamaschi, M., Aprea, E., Betta, E., Biasiolli, F., Cipolat-Gotet, C., Cecchinato, A., Bittante, G., Gasperi, F. *J. Dairy Sci*., 2015. 98, 2183-2196.
2. Gómez-Ruiz, J.Á., Ballesteros, C., Viñas, M.Á.G., Cabezas, L., Martínez-Castro, I. *Lait*, 2002. 82, 613-628.
3. Bintsis, T., Robinson, R.K. *Food Chemistry*, 2004. 88, 435-441.

Poster 42

The interaction between Ru/Os piano stool complexes and lysozyme impacts protein stability

Matthew P. Sullivan,[§†] Michael Groessl,[◊] Samuel M. Meier,[‡] Richard L. Kingston,[†] David C. Goldstone,[†] Christian G. Hartinger[§]

§ School of Chemical Sciences, University of Auckland, Private Bag 92019, Auckland, New Zealand
† School of Biological Sciences, University of Auckland, Private Bag 92019, Auckland, New Zealand
◊ TOFWERK, Uttigenstr. 22, Thun, Switzerland
‡ Institute of Analytical Chemistry, University of Vienna, Waehringer Str. 38, Vienna, Austria

Since the advent of cisplatin (1987),[1] there has been a fervent search for the next 'blockbuster' metal-based anticancer drug. This search led to the advent of the piano-stool scaffold which holds a number of favourable properties and with small changes to the ligand structures, significant changes in the biological activity were observed.[2] In order to investigate the impact of metalation of the model protein hen egg white lysozyme (HEWL) with M(η^6-p-cymene)X_2 (where M=Ru, Os. X=Cl, Br, I), we employed ion mobility mass spectrometry (IM-MS), differential scanning calorimetry (DSC), dynamic light scattering (DLS), and protein X-ray crystallography to characterise interactions.

Protein stability was detected with IM-MS, DSC, and DLS, which showed a greater effect for the ruthenium chlorido species over the other complexes tested. Crystal structures of metallated HEWL showed altering the metal centre/ligands changed the number of adducts formed. The ruthenium chlorido species was observed binding at two sites (Figs. 1a and 1b) while a simple exchange to bromido ligands or replacing the Ru with an Os centre showed binding only at the major site (Fig. 1a). The choice of metal centre and leaving group clearly impact the binding interactions of piano stool complexes.[3] Further investigative organometallic species, dichlorido(1,3-dimethylbenzimidazole-κC2)(η^6-*p*-cymene)ruthenium(II) and chlorido[N-(4-(maleimidyl)phenyl)pyridine-2-carbothioamide](η^6-*p*-cymene)ruthenium(II) chloride interactions were explored with HEWL, which show varying binding modalities due to their unique ligand structures (Fig. 1c).[4]

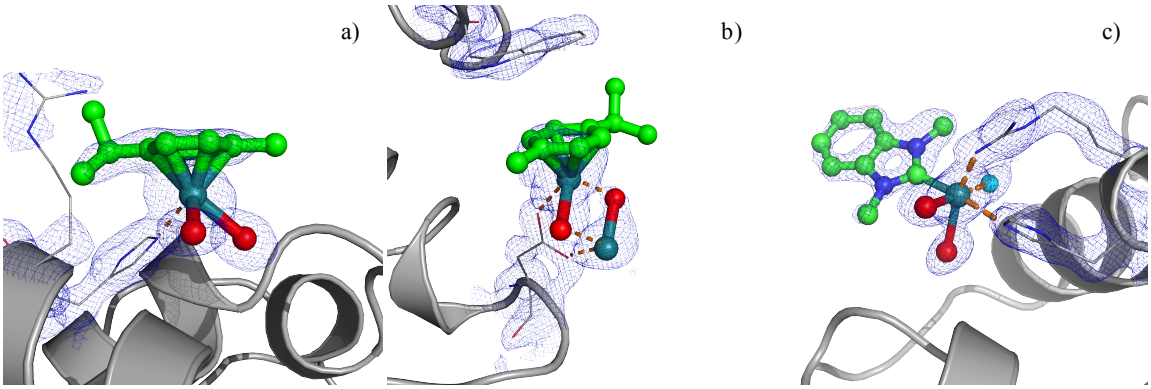

Figure 1. [M(cymene)Cl_2]$_2$ interactions with HEWL. a) Site 1 showing the M(cymene)Cl_2 fragment attached to His15 of HEWL. b) A point of interaction was observed where (cymene)$RuCl_2$Ru coordinated to Asp101. c) Investigational complex interacting with His15 and Arg14 in a bidentate modality to HEWL with a water molecule completing the co-ordination sphere.

1. Arnesano, F.; Natile, G. *Coordination Chemistry Reviews* **2009,** *253*, 2070-2081.
2. Peacock, A. F.; Sadler, P. J. *Chemistry - An Asian Journal* **2008,** *3*, 1890-9.
3. Sullivan, M.; Groessl, M.; Meier, S. M.; Kingston, R.; Goldstone, D.; Hartinger, C. *Chemical Communications* **2017**.
4. Hanif, M.; Moon, S.; Sullivan, M. P.; Movassaghi, S.; Kubanik, M.; Goldstone, D. C.; Söhnel, T.; Jamieson, S. M. F.; Hartinger, C. G. *Journal of Inorganic Biochemistry* **2016**.

Poster 43

Characterisation of bioactive grape and wine metabolites through a combined organic, analytical and computational approach

Shi Min Tan

Gregory Chass[a], David Barker and Bruno Fedrizzi

[a]*Queen Mary University of London, United Kingdom*

C13-norisoprenoids are carotenoid-derived aroma compounds responsible for the characteristic aroma and flavors of wine. The majority of C13-norisoprenoids present in grapes exist either as free volatiles or as non-volatile glycoconjugates. The glucosidic forms of these compounds can undergo either acid or enzymatic hydrolysis to trigger the release of free volatiles contributing to the wine aroma and flavors.[1,2] This research aims to investigate the glycosides of C13-norisoprenoids and the corresponding chemical pathways for their formation in grapevine leaves, grape berries and as wine metabolites.[3,4,5] A combined approach involving the total synthesis of megastigm-4-en-3,6,9-triol-9-O-glucoside, megastigm-4-en-3,6,9-triol-3-O-glucoside, 4,5-dihydrovomifoliol 9-O-β-D-glucopyranoside and 4,5-dihydrovomifoliol 3-O-β-D-glucopyranoside (**Figure 1**), will allow analysis of these molecules from natural sources using mass-spectrometry (MS). In addition, computational modelling by high-level quantum chemical modelling will provide complementary structural, energetic and dynamic details to support MS fragmentation mechanisms.

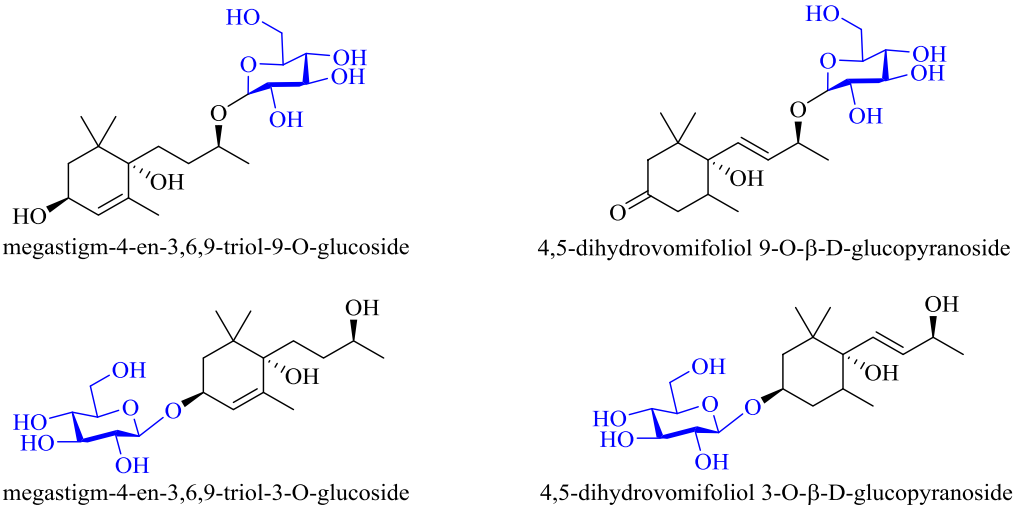

Figure 1. Glucosides in grapes and wines.

1. Williams, P. J.; Strauss, C. R.; Wilson, B.; Massy- Westropp, R. A. *Phytochemistry* **1982**, 21, 2013-2020
2. Günata, Y. Z.; Bayonove, C. L.; Baumes, R. L.; Cordonnier, R. E. *Journal of chromatography* **1985**, 331, 83-90
3. Teranishi, R.; Takeoka, G.; Güntert, M. *ACS Symp. Ser.* **1992**, 490(1), 1-6
4. Sefton, M. A.; Francis, I. L.; Williams, P. J. *Am. J. Enol. Vitic.* **1993**, 44, 359-370
5. Loscos, N.; Hernandez-Orte, P.; Cacho, J.; Ferreira, V. *J. Agric. Food Chem.* **2007**, 55, 6674-6684

Poster 44

Grape marc extract as an antioxidant and antimicrobial additive

Charlotte Vandermeer
Kenneth J. Olejar, Zoran Zujovic, Simon Swift[1], Paul Kilmartin
[1]*Department of Molecular Medicine and Pathology, University of Auckland*

Winery waste, or grape marc, is the skin, seeds, and stems left over from the wine-making process, and contains a high proportion of polyphenols, especially condensed tannins.[1] Incorrect storage of this waste can lead to environmental problems that have recently arisen in New Zealand.[2] A simple, environmentally friendly process was used to extract the phenolic compounds from the grape marc, which resulted in a brown powder. The resulting powder was heated to temperatures of 100, 150, 200, and 250 °C for a period of 10 minutes to establish the heat stability of the active compounds. For the extract to be considered as an additive in active packaging, it must be able to withstand high temperatures in the melt blending process. There was no significant loss in antioxidant or antimicrobial activity against *Staphylococcus aureus* or *Escherichia coli* after heating. The extract is not active against *Candida albicans*. Grape marc extract (GME) was therefore melt blended with high density polyethylene (HDPE) and linear low density polyethylene (LLDPE) at 170 °C, after which the resulting polymer underwent compression moulding to form thin films. Films containing 0.25% to 10% GME by weight were then characterised and their antioxidant and antimicrobial activity established.

1. Adams, D.O. *American Journal of Enology and Viticulture* **2006**, *57*, 249-256.

Poster 45

Reliable, Reproducible Detection for Accurate Measurement of Bovine Estrus and Pregnancy Using Centrifugal Microfluidics

Matheus J. T. Vargas, Mithileshwari Chandrasekhar, E. David Williams, M. Cather Simpson

Microfluidics is the science and technology of systems that process or manipulate small (10^{-9} to 10^{-18} litres) amounts of fluids, using channels in the micrometre range.[1] The replacement of a conventional pump with centrifugal force results in centrifugal microfluidics, also known as 'lab-on-a-disk'. Centrifugal microfluidics is a useful technique to develop automated or semi-automated sample-to-answer systems in micro total analysis.[2] The measurement of progesterone in cows is highly valuable for the dairy industry, and is currently the most widely accepted but not the most used measure for bovine oestrus and pregnancy. Current methods are based on observations of animal behaviour, and 5-15% of cows are inseminated when they are not in or near oestrus.[3] This research involves the construction of a reliable work station (**Figure 1**), fast and precise prototyping of centrifugal microfluidic disks, the development of hydrophilic and hydrophobic microfluidic valves, and detection methods. Finally, this research will enable full development and thorough characterization of an immunoassay-based sensor that can be deployed in a centrifugal microfluidic platform usable in the dairy industry.

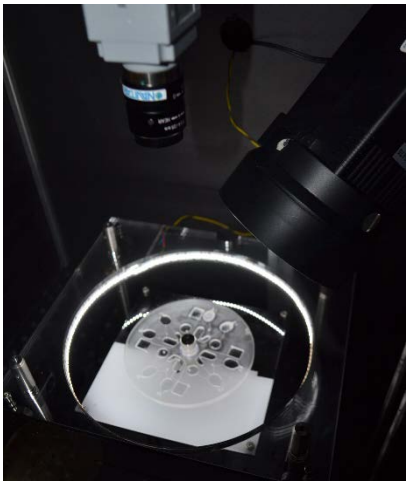

Figure 1. Centrifugal microfluidics working station.

1. George, M. W. *Nature* **2006**, *442* (7101), 368–373.
2. Strohmeier, O.; Keller, M.; Schwemmer, F.; Zehnle, S.; Mark, D.; von Stetten, F.; Zengerle, R.; Paust, N. Chem. Soc. Rev. 2015, 44 (17), 6187–6229
3. Pohler, K. G.; Green, J. A.; Geary, T. W.; Peres, R. F. G.; Pereira, M. H. C.; Vasconcelos, J. L. M.; Smith, M. F. In Regulation of Implantation and Establishment of Pregnancy in Mammals; Geisert, R. D., Bazer, F. W., Eds.; Springer International Publishing, 2015; Vol. 216, pp 253–270.

Poster 46

Laser scribed graphene/PVDF-HFP composite electrodes with improved mechanical water wear and their electrochemistry

Guangyuan Xu
Paul A. Kilmartin and Jadranka Travas-Sejdic

As a recent member in carbon nanomaterials, graphene has been widely investigated in sensing and energy applications due of its specific two-dimensional nanostructure and attractive intrinsic properties. Laser scribing of graphite oxide (GO) is a facile and cost-effective technology for fabricating patterned reduced graphene oxide electronics in a single-step. However, if the laser scribing does not occurs through all of the layers of the graphite oxide, the existence of water-soluble graphite oxide underneath the laser scribed graphene may result in the unexpected low-stability of the produced electronic elements in aqueous media. This study investigates the electrochemical performance and mechanical stability of laser scribed graphene films that contained various content of poly(vinylidene fluoride-co-hexafluoropropylene) as a binder, blended into the graphite oxide dispersion. The laser scribed composite graphene electrodes not only showed improved water mechanical wear resistance, but also largely unaffected the electrochemical behaviour when compared with the binder-free laser scribed graphene. The findings are significant in terms of the development of robust bioelectronics, to be employed in aqueous environments, based on the simple methodology of laser scribing of GO.

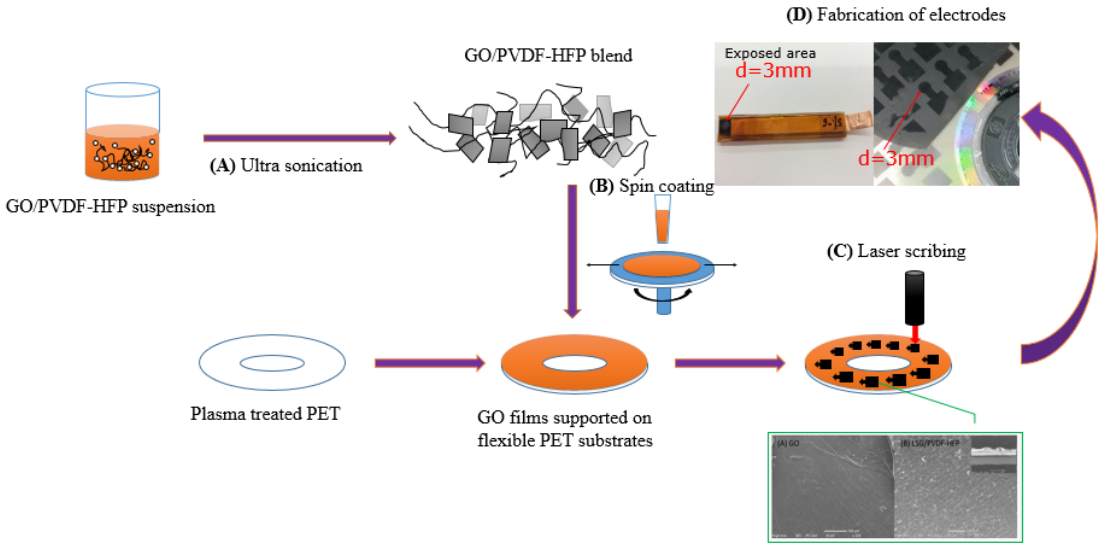

Figure 1. Schematic description of the laser scribing of graphite oxide/PVDF-HFP composite and the process of LSG/PVDF-HFP hybrid electrode preparation: (A) The dispersion of GO/PVDF-HFP in NMP by ultra-sonication; (B) Spin coating of the homogenous GO/PVDF-HFP solution onto a plasma treatment PET substrate ; (C) Direct laser writing of patterned LSG electrodes using a LightScribe DVD burner; (D) The individual electrodes (exposed area 3 mm in diameter) fabricated into a working electrode for the electrochemical experiments.

Poster 47

The identification of novel *Vitis vinifera* polyphenol oxidase inhibitors using virtual screening

Ayesha Zafar, Yu Li, Jóhannes Reynisson, Ivanhoe K. H. Leung

Vitis vinifera polyphenol oxidase (PPO) is a copper-containing enzyme that catalyses oxidation of phenolic compounds in grapes.[1] Polyphenol Oxidase (PPO)[2-4] protein represents a new target to improve the shelf life of fruits but suitable inhibitors are lacking. Therefore, in order to identify active compounds (hits) virtual high throughput screening was performed. A screen was performed using approximately $1^{\times}10^4$ natural products. These were screened against the binding pocket of PPO (PDB:2p3x, Resolution: 2.2 Å)[1] using GOLD. As a result **34** plausible compounds were identified (virtual hits). Then, the ^{1}H NMR-based single concentration inhibition experiments were conducted. Interestingly, a reduction of grape PPO catalytic activity was observed for almost all compounds. However, most were found to be weak inhibitors and only showed around 20% reduction in catalytic activity as compared to known inhibitor Tropolone. Two compounds, **16** and **26**, led to a ~40% reduction in grape PPO catalytic activity, which is similar to other reported PPO inhibitors including Morin and 2,4-dihydroxycinnamic acid. Importantly, unlike many reported PPO inhibitors, our compounds do not contain the phenol or diphenol scaffold. Furthermore, In order to explore the chemical space around Tropolone for activity against PPO, six close structural analogues were selected using molecular modelling and tested using the ^{1}H NMR-based assay. Interestingly, it revealed another active compound **7** which is found to be a stronger inhibitor than Troplone with an IC_{50} value of 2μM (Figure 1).

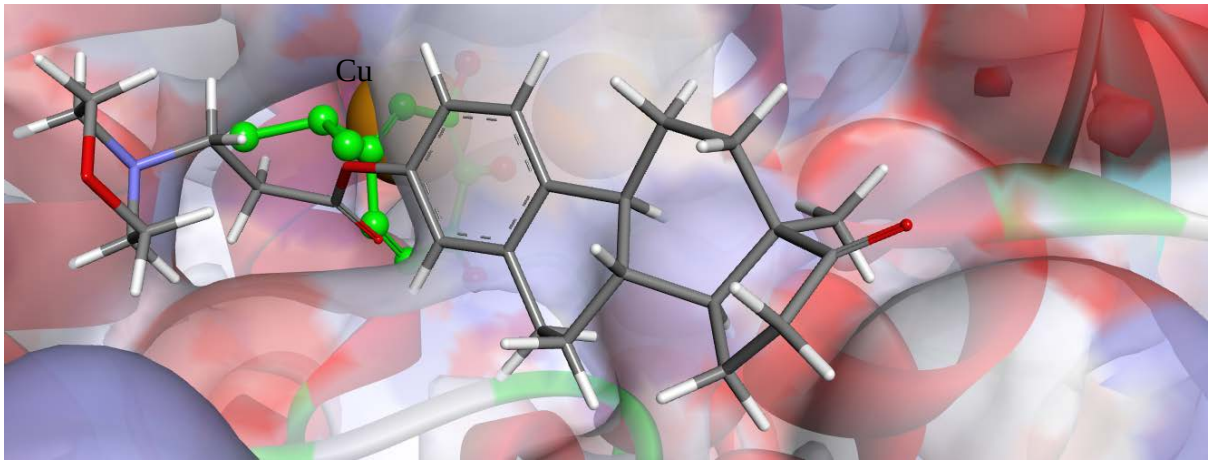

Figure 1. The docked configuration of compound **7** and **16** to the binding site of PPO (PDB:2p3x) using GS and PLP. The protein surface is rendered. Red depicts a positive partial charge on the surface, blue depicts negative partial charge and grey shows neutral/lipophilic areas. Compound **7** (Green ball and stick) fits into the binding site while compound **16** (stick) sits in front of the pocket.

1. V. M. Virador, J. P. Reyes Grajeda, A. Blanco-Labra, E. Mendiola-Olaya, G. M. Smith, A. Moreno and J. R. Whitaker, *Journal of agricultural and food chemistry*, 2009, **58**, 1189-1201.
2. P. Nokthai, V. S. Lee and L. Shank, *International journal of molecular sciences*, 2010, **11**, 3266-3276.
3. H. Wang, S. Yan, Q. Wang and S. H. J. Li.
4. S. Raghavendra, S. J. A. Rao, V. Kumar and C. K. Ramesh, *Computational biology and chemistry*, 2015, **59**, 81-86.

Poster 48

Morphology of noni juice containing maltodextrin and gum acacia during single droplet drying

Chuang Zhang[1]

Nan Fu[2], Xiao Dong Chen[2], Siew Young Quek[1]*

[1] *Food Science, School of Chemical Sciences, The University of Auckland, Auckland, New Zealand*.

[2] *School of Chemical and Environmental Engineering, College of Chemistry, Soochow University, Suzhou, China*.

Microencapsulation of noni juice by spray drying masks its unpleasant odour and also protects bioactives which are sensitive to environment.[1] In this study, noni juice was encapsulated with maltodextrin (MD) and gum acacia (GA). Single droplets of noni juice with different compositions were suspended on a glass filament to observe the drying and dissolution behaviours. At each drying stage, the drying process was stopped to investigate changes occurred in the morphology of semi-dried particle, either by attaching an additional water droplet or by maintaining the semi-dried/dried particle suspended in a convective drying chamber with no air flow. By conducting the test, the morphology changes were compared at various drying stages. The microstructures of dried particles were observed by scanning electron microscopy (SEM), and the morphologies were compared by observing its surface and inner microstructures. The results obtained in this investigation show the underlying mechanisms of particles formations during single droplet drying of noni juice containing MD and GA.

1. Gharsallaoui, A., Roudaut, G., Chambin, O., Voilley, A., & Saurel, R. (2007). Applications of spray-drying in microencapsulation of food ingredients: An overview. *Food Research International*, *40*(9), 1107-1121.

Poster 49

Antimicrobial Polymer and Surface Modification

Qiang Zhang[1,2,3], Mona Damavandi[1,2], David Barker[2], Simon Swift[3], Ralph Cooney[2,3], Jadranka Travas-Sejdic[1,2,3]

[1] Polymer Electronic Research Center, [2]School of Chemical Science, University of Auckland, New Zealand.
[3] Biocide Toolbox, University of Auckland, New Zealand.

As one of the oldest and the most successful life forms on earth, micro-organisms possess versatile and efficient adaptive mechanisms which allow them morphing or evolving to survive extreme conditions including antibiotics that have been widely used since penicillin. To restrain the constantly evolving bacteria strains and consequently resistance to present antibiotics, novel antimicrobial agents and methods are in great demand. Conjugated polymers have been proven to be antimicrobial due to reactive oxygen species generated under light activation.

Conjugated polymers, such as poly(*p*-phenylene vinylene), poly(*p*-phenylene ethynylene), have been studied to create physical damage to the bacteria membrane, organelles and enzymes.[1] The antimicrobial efficiency is largely controlled by properties of the conjugated system, as well as pendants or side chains along the polymer. Poly(thiophene phenylenes) (PThP) is another novel conjugated polymer which could be modified further with a range of functional groups.[2] From this research specifically, side chains of quaternary ammonium salts which afford another mechanism of highly efficient biocide have been grafted from the PThP by Activator ReGenerated by Electron Transfer Atom Transfer Radical polymerization (ARGET-ATRP).

1. Ji, E.; Corbitt, T. S.; Parthasarathy, A.; Schanze, K. S.; Whitten, D. G. *ACS applied materials & interfaces* **2011,** *3*, 2820-2829.
2. Chan, E. W. C.; Baek, P.; Barker, D.; Travas-Sejdic, J. *Polymer Chemistry* **2015,** *6*, 7618-7629.

Poster 50

Synthesis and Biological Evaluation of Callyearin A and Its Analogues as Potential Anti-TB Therapeutics

Shengping Zhang
Luis M. De Leon Rodriguez, Paul W. R. Harris, Greg Cook, Margaret A. Brimble

Mycobacterium tuberculosis (*Mtb*) is the causative agent of tuberculosis (TB), an infection considered as a global public health emergency given its high prevalent mortality and morbidity. Callyaerin **A**, a naturally occurring cyclic peptide that contains an unusual (*Z*)-2,3-diaminoacrylic acid moiety, has recently been shown to exhibit potent activity against *Mtb* (MIC_{90}, 2.0 μM) with no observed cytotoxicity.[1-3] Therefore, the syntheses of callyearin **A** and its analogues are carried out using solid phase peptide synthesis strategy in order to explore their potential as new drug leads for the treatment of TB. Briefly, an acetal protected formyl glycine was introduced into the sequence to afford the corresponding side chain aldehyde functionality after the acid-mediated peptide cleavage. The formation of the enamine linkage between isoleucine and the formyl glycine then quickly occurred through the condensation between the *N*-terminal amine and the generated aldehyde after the treatment of the linear peptide with 0.1% TFA in acetonitrile. Finally, callyearin **A** was obtained in a high yield (>90%) and the remaining analogues are now being prepared in the same fashion. All the synthetic peptides will be tested for their anti-TB activity in order to gain further knowledge on the structure-activity relationships of this family of peptides.

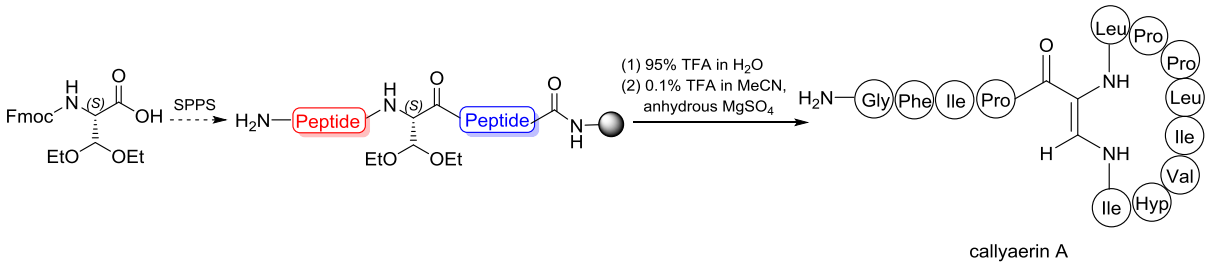

Figure 1. Synthesis of the callyaerin A.

1. Ibrahim, S. R. M.; Min, C. C.; Teuscher, F.; Ebel, R.; Kakoschke, C.; Lin, W.; Wray, V.; Edrada-Ebel, R.; Proksch, P. *Bioorg. Med. Chem.*, **2010**, *18*, 4947-4956.
2. Daletos, G.; Kalscheuer, R.; Koliwer-Brandl, H.; Hartmann, R.; De Voogd, N. J.; Wray, V.; Lin, W.; Proksch, P. *J. Nat. Prod.*, **2015**, *78*, 1910-1925.
3. De Leon Rodriguez, L. M.; Kaur, H.; Brimble, M. A. *Org. Biomol. Chem.*, **2016**, *14*, 1177-1187.